Turk J Chem
28 (2004) , 587 – 601.

Electrorheological Properties of Suspensions Prepared from Poly(Li-tert-butyl methacrylate) Ionomer

Mustafa YAVUZ
Süleyman Demirel University, Science and Arts Faculty, Chemistry Department
32200 Isparta-TURKEY
Halil İbrahim ÜNAL*
Gazi University, Science Faculty, Chemistry Department, Teknikokullar,
06500, Ankara-TURKEY
e-mail: hiunal@gazi.edu.tr

Received 04.08.2003

The synthesis, characterisation and partial hydrolysis of poly(tert-butylmethacrylate), (PTBMA), and the electrorheological (ER) properties of its suspensions were investigated. The polymer was synthesised by radical polymerisation and partially hydrolysed by para-toluenesulphonic acid monohydrate ($PTSA.H_2O$), and then converted to a lithium salt (PTBMA-Li) by washing with a $LiOH_{(aq)}$ solution. From particle size measurements, the average particle size of PTBMA-Li was determined to be 74 μm. Colloidal suspensions of ionomer were prepared in various insulating oils [silicone oil (SO), mineral oil (MO), threeoctylthreemellitate (TOTM) and dioctylphatalete (DOP)] at a series of concentrations (c = 5-33 m/m, %). The sedimentation stabilities of these suspensions were determined at 20 °C and were observed to increase with decreasing suspension concentration. Maximum gravitational stability was observed as 32 days in SO at c = 5 m/m, %. Flow times of suspensions were measured under no applied electric field (E = 0 kV/mm), and under an external electric field (E $\neq$ 0 kV/mm), and ER activity was determined. The highest flow time was found to be 32 s in SO at c = 33 m/m, %. Further, the effects of solid particle concentration, shear rate ($\dot{\gamma}$), electric field strength, (E) addition of polar promoters and high temperature on the ER activities of colloidal suspensions were investigated. Excess shear stresses ($\Delta\tau$) were determined to be 74 Pa under E = 1.0 kV/mm.

Key Words: Electorheological fluids, poly(tert-butylmethacrylate), ionomer, colloidal dispersions.

Introduction

Electrorheological (ER) fluids are made of an insulating liquid medium and polar dispersed particles. ER fluids undergo a rapid reversible transition from a liquid to a solid in milliseconds, and exhibit a high yield stress and viscosity on the application of an external electric field (E). The yield stress and electric field viscosity ($\eta_{E\neq0}$) could reversibly be changed by several orders of magnitude under an external electric field

*Corresponding author

with the strength of several kV/mm. This change is known to be due to the migration of polar particles and the formation of chain-like or fibrillar structures oriented in the electric field direction over the gap between the electrodes. This orientation is due to the mismatch of dielectric constant of the dispersed particles and the insulating oil under a high external electric field[1−3].

ER fluids, as a kind of smart material, may possibly be revolutionary in several areas of industry such as the clutch, brake and vibration damper in the automotive industry, the arm and hand joints in robotics, and for military purposes[4−8]. Several comprehensive reviews on this subject have been reported in the literature[1,2,9]. Corn starch, silica, cellulose and zeolite[10−12] have been widely used as the disperse phase in the formulation of hydrous (wet-base) ER fluids, which have several problems related to durability, limited temperature range and colloidal instability.

Recently, special attention has been paid to unhydrous (dry-base) ER fluids (which do not contain any polar solvent in the disperse phase). Examples include poly(acenequinone) radicals[13,14], homopolyaniline[15,16], copolyaniline[17,18], poly(phenylene diamine)[19], polyurethane[20], and polymer-clay nano-composites of styrene-acrylonitrile copolymer[21,22] or polyaniline[23,24].

The carrier species of the polarised particles is the main difference between dry- and wet-base ER fluid systems. In wet ER fluids, the fibrillar structure is formed as a result of the migration of ionic particles in the absorbed water, whereas in dry ER fluids, electronic migration inside the molecules of the dispersed particles is the driving force behind the particle-chain structure. Both affect the ER and the magnitude of yield stress under an applied electric field.

To overcome some of the limitations mentioned above, ion-containing polymers (ionomers) are chosen as a disperse phase, because they receive ever-increasing attention attributed to the dramatic effect that small amounts of ionic groups exert on ultimate polymer properties. After the incorporation of ionic groups into the polymer backbone, the tensile strength, melting solution viscosity, glass transition temperature and rheological properties of the main polymer change and this makes them useful for ER studies[25−27].

In this research PTBMA-Li was synthesised as a new disperse phase and a potential candidate for dry-base particles, and the rheological and electrical properties pertaining to the ER of PTBMA-Li suspensions were investigated in various insulating oils. The results are also compared with the sedimentation stability and ER activity data obtained from polyisoprene-co-poly(Li-tert-butylmethacrylate), PI-co-PTBMA-Li/silicone oil system, which we studied earlier[28].

Experimental

Materials

Methacrylic acid and toluene were purified by vacuum distillation. Benzoylperoxide (BP) was recrystallised from methanol and dried in a vacuum oven for 48 h. Tert-butylmethacrylate was synthesised in our laboratory. All the other chemicals were (Aldrich, analytical grade) used as received.

Polymerisation

Firstly the monomer, tert-butylmethacrylate, was synthesised as follows: 1.89 mol methacrylic acid was chlorinated with equimolar $SOCl_2$(l) at 80 °C and methacrylic acid chloride was obtained with 94% yield and the product was purified by distillation. This product was subjected to an esterification reaction with

tert-butylalcohol at 25 °C and tert-butylmethacrylate (TBMA) was recovered with 83% yield. TBMA was purified by washing with $NaHCO_3$(aq) solution and then distilled water, respectively. Then it was filtered through a molecular sieve. Further, to remove any remaining impurities, it was distilled under vacuum (0.01 mmHg). The purity of TBMA was checked by thin layer chromatography.

After synthesising TBMA, poly(tert-butylmethacrylate) (PTBMA) was prepared by radical polymerisation in toluene using BP as an initiator at 80 °C, under $N_{2(g)}$ atmosphere. The polymer was precipitated in excess methanol and dried in a vacuum oven at 50 °C before the hydrolysis reaction. The reaction mechanisms for the synthesis of TBMA and PTBMA are described in Scheme.

Monomer synthesis

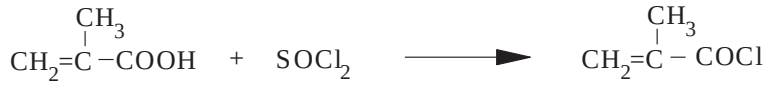

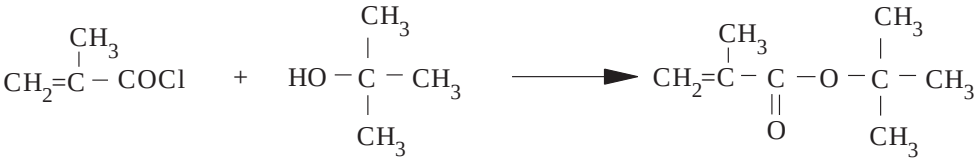

Polymerisation

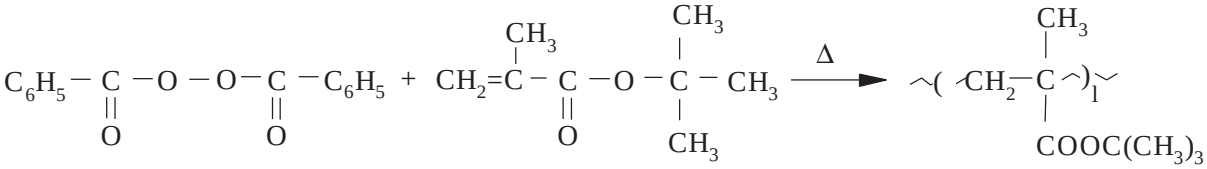

Hydrolysis

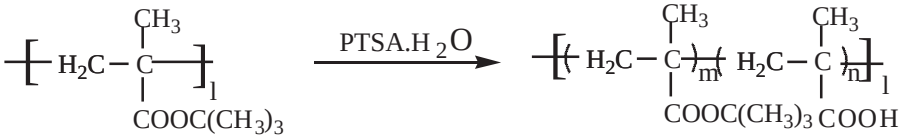

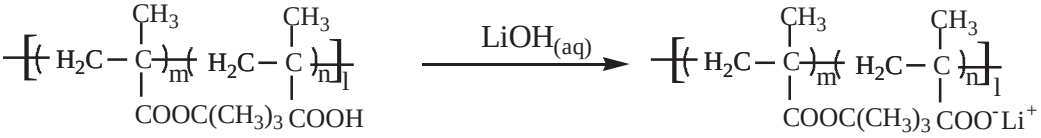

where m = 25.75, n = 2.25 and l = (m + n) = 28

Scheme. Synthesis, partial hydrolysis and salt formation reaction mechanisms of PTBMA.

Hydrolysis reaction

To form an ER active material from PTBMA it needs to be partially hydrolysed to carboxylic acid units and converted to a lithium salt. The polymer was dissolved in toluene and PTSA.H_2O was added to this solution, followed by stirring under $N_{2(g)}$ atmosphere for 30 min. The solution was then transferred to a separating funnel and washed with 100 cm^3 of 0.1 M $LiOH_{(aq)}$ to remove residual PTSA.H_2O from the reaction medium. This organic phase was also washed with distilled water to remove any residual $LiOH_{(aq)}$. The product was dried in a vacuum oven at room temperature for at least 72 h. The reaction mechanism for the partial hydrolysis of PTBMA and the formation of lithium salt are described in Scheme.

Characterisation

End group analysis was performed to determine the molar mass of the polymer (M_n), by titrating ester units of the polymer with 0.1 M $NaOH_{(aq)}$.

Intrinsic viscosity was measured in toluene using a Ubbelohde capillary flow viscometer mounted in a water bath maintained at 25.00 ± 0.01 °C.

The ^{1}H-NMR spectrum was obtained in DMSO-d_6 at ambient temperature using a 400 MHz Bruker DPX Avonce Nuclear Magnetic Resonance Spectrometer at the Scientific and Technical Research Council of Turkey (TUBITAK) research laboratory.

The FTIR spectrum of the polymer was recorded using a Mattson Model 1000 spectrometer. Samples were analysed as films cast from dichloromethane onto a sodium chloride plate.

Elemental analysis was performed by TUBITAK's microanalytical laboratory, and the results were used to check purity by comparison with the calculated composition.

The particle size of the ionomer (PTBMA-Li) was determined by Fraunhafer scattering using a Malvern Mastersizer E, version 1.2b particle size analyser. The ionomer was dispersed in distilled water and stirred at a constant temperature of 20 °C. The data collected were evaluated by the Malvern software computer according to Fraunhafer diffraction theory[29]. The average diameter of the ionomeric particles was determined to be 74 μm.

Preparation of suspensions

Colloidal suspensions of the ionomer were prepared in 4 insulating oils at a series of concentrations (c = 5-33 m/m, %) by dispersing a definite amount of the ionomer in a calculated amount of insulating oil according to the formula;

$$(m/m, \%) = [m_{\text{polymer}}/(m_{\text{polymer}} + m_{\text{oil}})] \times 100 \quad (1)$$

Determination of sedimentation stability of PTBMA-Li suspensions

The sedimentation stability of ionomeric suspensions, prepared at c = 5-33 (m/m, %) concentrations, was determined at 20 °C. Glass tubes containing the suspensions were immersed in a constant temperature water bath and the formation of the first precipitates at the bottom of the tubes was taken to indicate colloidal instability.

Electrorheological measurements

Electrorheological measurements were carried out for the ionomeric suspensions prepared in 4 insulating oils, for the experimental determination of flow and visco-elastic material properties, under an external applied electric field, which influences processing technology and the polymer's stability and consistency.

Flow measurements

Flow rate measurements were carried out between 2 brass electrodes at 20 °C for the ionomeric suspensions prepared in 4 insulating oils. The gap between the electrodes was 0.5 cm, the width of the electrodes was 1.0 cm and the height of liquid on the electrodes was 5.0 cm. During the measurements, these electrodes were connected to a high voltage dc electric source and a voltmeter.

At the beginning of the experiment, the electrodes were dipped into a vessel containing the ER fluid and after a few seconds the vessel was removed and the flow time for complete drainage measured using a digital stopwatch. At the second stage, the electrodes were again dipped into the same vessel containing the ER fluid and a high voltage was applied above the yield point, perpendicular to flow direction. After several seconds the vessel was removed and the flow time for complete drainage measured under the applied electric field ($E \neq 0$ kV/mm). This procedure was repeated for each ER fluid concentration under various field strengths.

Rotational viscometry

To observe the ER effect of ionomeric suspensions, rotational viscometry (Brookfield DV-1+, Brookfield Instruments) was carried out at 2 different temperatures, 20 °C and 80 °C. The shear rates applied were relatively low (0.1-20 s^{-1}), due to instrumental limitations. To measure the viscosity of a suspension, a spindle was simply immersed in the liquid container, the motor was switched on and the viscosity was read on the calibrated dial of the instrument. For measuring the viscosity of suspensions under an external applied electric field, those parallel plate electrodes were immersed into the fluid container, an electric field was created in the fluid perpendicular to the parallel plates and the spindle was forced to rotate. During the experiments the gap between the brass electrodes was kept constant at 5 cm. The voltage used was supplied by a 0-10 kV (with 0.5 kV increments) dc electric field generator, which enabled electric field induced polarisation to be created during the experiments.

Results and Discussion

Characterisation

Characterisation of the PTBMA and PTBMA-Li is discussed below. The equivalent number average molar mass of PTBMA was determined to be 3700 g/mol from the end group analysis.

Intrinsic viscosities of PTBMA and PTBMA-Li were determined by extrapolating to infinite dilution from plots of $\ln\eta_r/c$ and η_{sp}/c against concentration and found to be 0.20 dm^3/g and 0.12 dm^3/g, respectively. It was observed that the polymeric salt reached a lower zero field viscosity ($\eta_{E=0}$) after partial hydrolysis and salt formation.

Chemical shifts of particular functional groups in PTBMA, obtained from ^{1}H-NMR, are given in Table 1.

Table1. Chemical shifts obtained from PTBMA by ^{1}H-NMR in DMSO-d_6.

Assignment	Chemical shifts (δ, ppm)
-C(CH_3)$_3$	2.2
-CH_3	2.4
-CH_2	3.4

The FTIR spectrum of PTBMA showed the expected distinctive absorptions. The absorptions at 2920 cm^{-1}, 1740 cm^{-1}, 1600 cm^{-1}, 1400 cm^{-1} and 1240 cm^{-1} are typical of C-H bending due to CH_3 absorptions, -C=O stretchings, ether stretching due to C-O-C, aliphatic C-H stretching, and C=C stretching, respectively. The hydrolysed copolymer gave a similar FTIR spectrum to PTBMA with an additional peak at 3400 cm^{-1}, due to O-H binding.

The experimental and calculated compositions obtained from elemental analysis of the PTBMA and PTBMA-Li are given in Table 2. The measured compositions agree very well with the calculated values. These results also prove that the PTBMA is successfully partially hydrolysed and converted to the Li salt.

Table 2. Elemental analysis results of PTBMA and PTBMA-Li.

		C (%)	H (%)	O (%)	Li (%)
PTBMA	Calculated	67.8	9.9	22.3	-
	Found	66.6	9.1	21.6	-
PTBMA-Li	Calculated	68.0	9.8	21.8	0.4
	Found	67.9	9.7	22.0	0.4

Sedimentation stability of PTBMA-Li suspensions

The sedimentation stability of PTBMA-Li suspensions was determined in 4 insulating oils at 20 °C and the results obtained are tabulated in Table 3. The sedimentation stability of suspensions decreased with increasing ionomer concentration. The maximum sedimentation stability was 32 days in SO at c = 5% ionomer concentration. The highest and lowest sedimentation stabilities of suspensions were obtained in SO and DOP as 32 days and 2 h, respectively. The results indicate that SO forms a better dispersion medium than the other insulating oils, which may be attributed to the dielectric constant difference (see Table 4).

Table 3. Sedimentation stability results of PTBMA-Li in various oils. (T = 20 °C)

Dispersion medium	Concentration (m/m)					
	33%	25%	20%	15%	10%	5%
SO	13 days	15 days	16 days	20 days	25 days	32 days
MO	5 days	7 days	9 days	11 days	15 days	27 days
TOTM	12 h	12 h	20 h	1 day	1 day	2 days
DOP	5 min	7 min	12 min	30 min	1 h	2 h

Table 4. Physical properties of insulating oils.

Oil	Boiling Point (°C)	Density (g/mL)	Dielectric Constant	Viscosity (Pas)
SO	>140	0.963	3.2	0.08
TOTM	163-165	0.821	-	0.08
DOP	384	0.981	5.1	0.04
MO	>110	0.862	2.2	0.04

The sedimentation stability of poly(isoprene)-co-poly(Li-tert-butyl methacrylate) ionomeric copolymer was also studied in our laboratory and found to be 57 days in SO at again c = 5% ionomer concentration[28]. We think that the amphiphilic copolymer formed a micellar structure in SO and showed higher resistance against gravitational forces and sedimentation.

Electrorheology

Flow measurements

Flow times of PTBMA-Li suspensions, prepared in SO at the range of c = 5-33 % concentrations, measured between the parallel plate electrodes at zero applied field (E = 0 kV/mm) and under various applied electric field strengths (E = 0-1.2 kV/mm) are shown in Figure 1. The flow times of suspensions increased with increasing electric field strength and suspension concentration. The highest flow time was obtained from c = 33% suspension in SO at E = 0.8 kV/mm as 32 s. The flow times illustrated in Figure 1 are the maximum flow times which could be measured under E = 1.2 kV/mm. When E was further increased, flow of the liquid between the electrodes stopped completely and measurement was not possible even after several hours. The same measurements were carried out for the suspensions prepared in the other 3 insulating oils and similar trends were observed. The maximum flow times of suspensions varied in the following order: SO (32 s) > MO (25 s) > TOTM (21 s) > DOP (15 s).

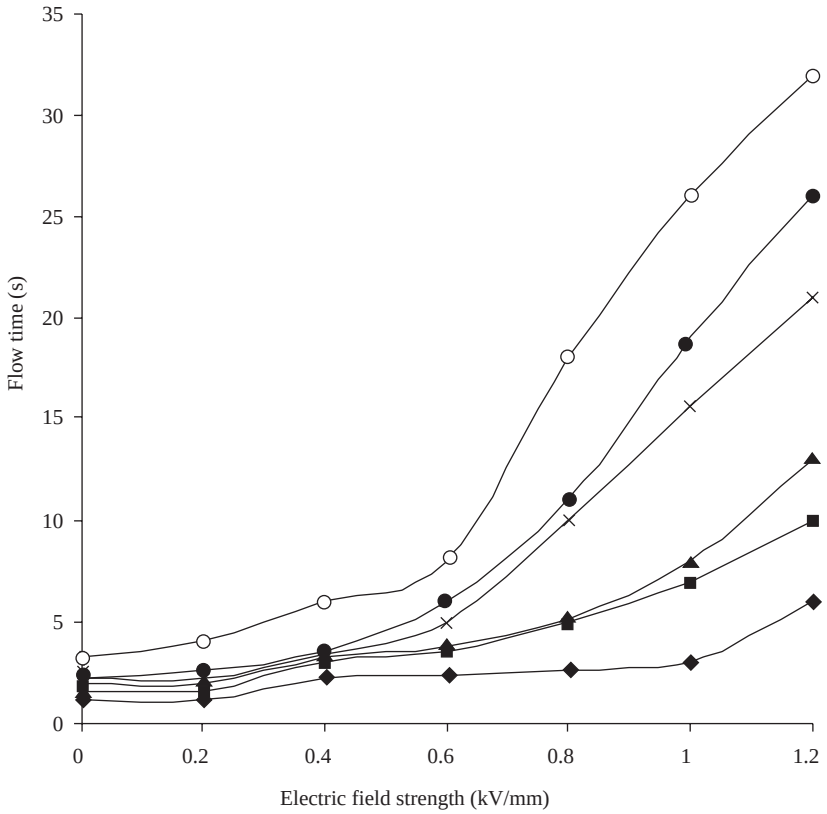

Figure 1. The changes in flow times with electric field strength.
Dispersion medium: SO, c (m/m, %): (♦) 5, (■) 10, (▲) 15, (×) 20, (●) 25, (◯) 33.

The differences between the flow times of suspensions in different insulating oils may be attributed to: (a) differences between the physical properties of the insulating oils such as density, viscosity and dielectric constant (see Table 4[30]), and (b) different intermolecular interactions acting between these insulating oils and the ionomer particles. It was observed that the occurrence of solidification and the observation of ER behaviour (non-Newtonian) shifted to low electric field strengths as the particle concentration was increased for all the suspensions studied ($E_{threshold}$ = 0.6 kV/mm for c = 20, 25 and 33% and $E_{threshold}$ = 1.0 kV/mm for c = 5, 10 and 15 %).

Similar behaviour was observed for the PI-co-PTBMA-Li/SO system and a 51 s flow time was recorded (c = 33%, E = 1.2 kV/mm)[28].

Results obtained from rotational viscometry

Effect of particle concentration on electric field viscosity

Figure 2 shows the changes in electric field viscosity ($\eta_{E\neq0}$)/zero field viscosity ($\eta_{E=0}$) with suspension concentration in silicone oil at various shear rates ($\dot{\gamma}$ = 0.1-20 s^{-1}). Up to 20% ionomer concentration, the viscosity ratio increases with increasing ionomer concentration. This trend is due to the polarisation forces acting between the ionic particles. The magnitude of this polarisation force (F) in the direction of the applied electric field (E) is[31]

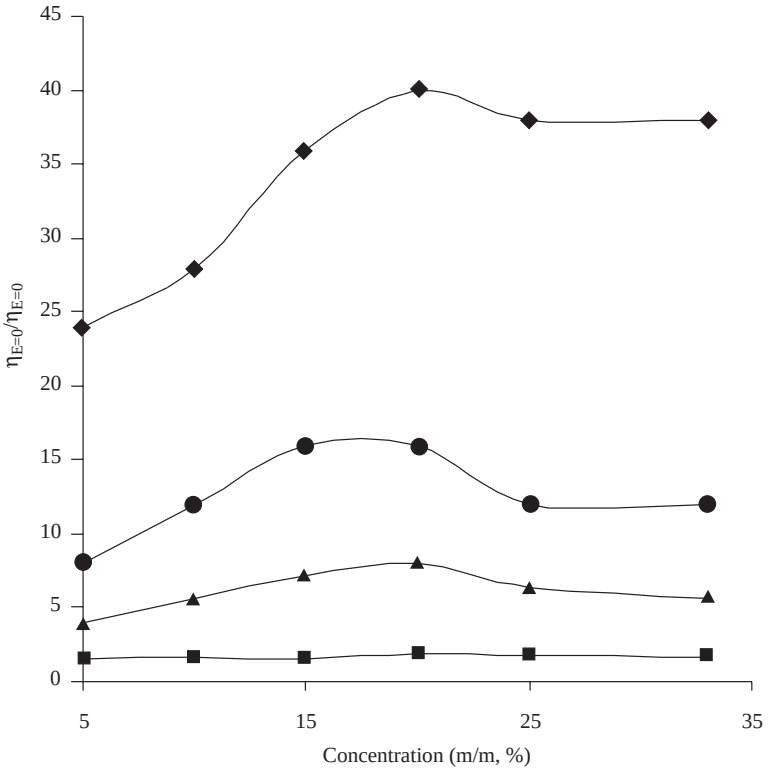

Figure 2. The changes in viscosity with concentration.
T = 20 °C, E = 0.0 and 1.0 kV/mm, dispersion medium: SO, $\dot{\gamma}$ (s^{-1}): (♦) 1, (●) 4, (▲) 10, (■) 20.

$$F = 6\varepsilon_2 r^6 E^2/\rho^4 \tag{2}$$

where $\varepsilon_2$is the dielectric constant of the particle, ρ is the distance between the particles, and r is particle radius.

As reflected in equation (2), the distance between particles decreases with increasing suspension concentration, which results in increased polarisation force and $\eta_{(E\neq 0)}$. When the particle concentration increases further above c = 20%, $\eta_{(E\neq 0)}$ decreases. This may be attributed to the following reasons: (a) at the higher ionomer concentrations, particles are closer to each other and electric double layers around particles overlap, and (b) the mutual action between the particles increases, and the electric double layers may drop out of particles.

Similar behaviours were reported by Yavuz and Unal[28], Wu and Shen[32], Kordonsky et al.[33] and Gow and Zukoski[34] in ER studies of PI-co-PTBMA-Li/silicone oil, chitin and chitosan/silicone oil, carboxymethyl cellulose/transformer oil and polyaniline/silicone oil systems, respectively.

Effects of electric field strength and shear rate on viscosity

Electric field strength against viscosity obtained at c = 20% optimum ionomer concentration in silicone oil is shown in Figure 3. At the beginning, η increases linearly with E^2, whereas, at higher values of E, after the application of required threshold energy, a transition to a linear relationship between η and E takes place. For $\dot{\gamma}$ = 0.1 and 0.4 s^{-1}, this critical field strength (or threshold energy) is 0.4 kV/mm, and for $\dot{\gamma}$ = 1, 10 and 20 s^{-1}, the critical field strength rises to 0.6 kV/mm. This may be attributed to the increased magnitude of electric field induced dipole-dipole interactions and polarisation forces[35]. As reflected in the graph, this transition is shear rate dependent.

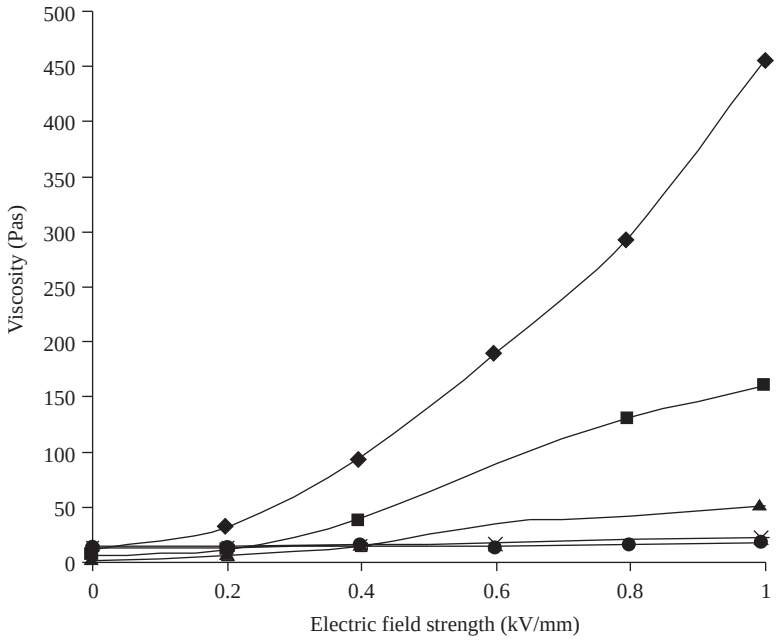

Figure 3. The changes in viscosity with electric field strength.
T = 20 °C, c = 20%, dispersion medium: SO, $\dot{\gamma}$ (s^{-1}): (♦) 0,1, (■) 0,4, (▲) 1, (×) 10, (●) 20.

Under an applied shearing force, particles were also affected by viscous forces, due to the hydrodynamic interactions of particles in the suspension. The magnitude of these viscous forces is[32]

$$F = 6\pi\eta_s r^2\dot{\gamma} \tag{3}$$

where η_s is the viscosity of the suspension, r is the particle radius, and $\dot{\gamma}$ is the average shear rate. On the other hand, at higher shear rates ($\dot{\gamma}$ = 10 and 20 s^{-1}) η_s became independent of E. This is because at high shear rates the viscous forces become dominant and the fibrillar structure of the suspension does not vary with E.

Similar results were reported by Yavuz and Unal[28], Yang and Huang[36] and Lengalova et al.[37] for ER studies of PI-co-PTBMA-Li/silicone oil, poly(n-hexyl isocyanate)/o-xylene and polyaniline/silicone oil systems, respectively.

Changes in excess shear stress with concentration

The effect of suspension concentration on excess shear stress ($\Delta\tau = \tau_{E\neq0}$-$\tau_{E=0}$) was studied at $\dot{\gamma}$ = 20 s^{-1}, T = 20 °C and E = 0 and 1 kV/mm constant conditions**.** It is seen from Figure 4 that $\Delta\tau$ increases with increasing ionomer concentration up to c = 20 %, reaches a maximum and then almost levels off in all the dispersion media examined. The highest $\Delta\tau$ was obtained in SO as 35 Pa, while the lowest was in MO, which may be attributed to the formation of swollen and shrink ionomer structures in SO and MO, respectively. $\Delta\tau$ = 43 Pa was obtained for the PI-co-PTBMA-Li/silicone oil system[28] under the same conditions, which indicates the formation of a stronger electric field induced particle-chain structure under an applied field. Generally, the increase in $\Delta\tau$ was due to the increased polarisation forces as the particle concentration was increased, which results in enhanced ER activity. These secondary forces may be stronger in the PTBMA-Li/SO system than in the others. It was found that the shear stress of the ER suspension was largely dependent on the particle concentration. A similar trend was reported by Wu and Shen[32] for chitin/SO and a chitosan/SO system, and by Yin and Zhao[38] for a glycerol activated titania/SO system. A linear relationship between shear stress and particle concentration was derived, on the basis of a fibrillation model, by Klingenberg and Zukoski[39]. Block[13] and Xu[40] reported that shear stress parabolically increases with particle concentration. However, Bossis et al.[41] observed that shear stress passes through a maximum as particle concentration increases. Hao[6] reported that critical particle concentrations show changes depending on the types of ER suspension systems under investigation.

Changes in excess shear stress with electric field strength

Figure 5 represents the changes in $\Delta\tau$ with E. As reflected in the graph, $\Delta\tau$ increases with rising E for all the insulating oils studied but this increase is particularly sharp in silicone oil medium. This indicates that ER suspensions form a stronger fibrillar structure under increasing electric field strength. Similar behaviour was observed for the PI-co-PTBMA-Li/silicone oil system in our previous study[28] and has also been reported for various other ER fluid systems such as glycerol activated titania/silicone oil[38], water doped microcrystalline cellulose/mineral oil[42] and poly(naphthalene quinone) radical/silicone oil[43].

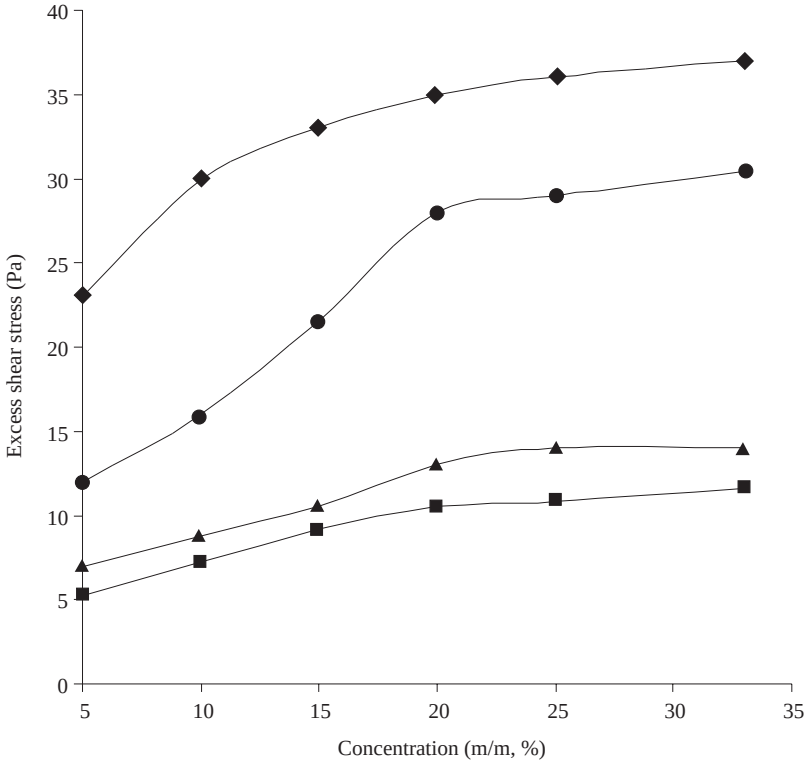

Figure 4. The changes in excess shear stress with concentration.
$\dot{\gamma} = 20\ s^{-1}$, T = 20 °C, E = 0.0 and 1.0 kV/mm, dispersion medium: (♦) SO, (▲) TOTM, (■) MO, (●) DOP.

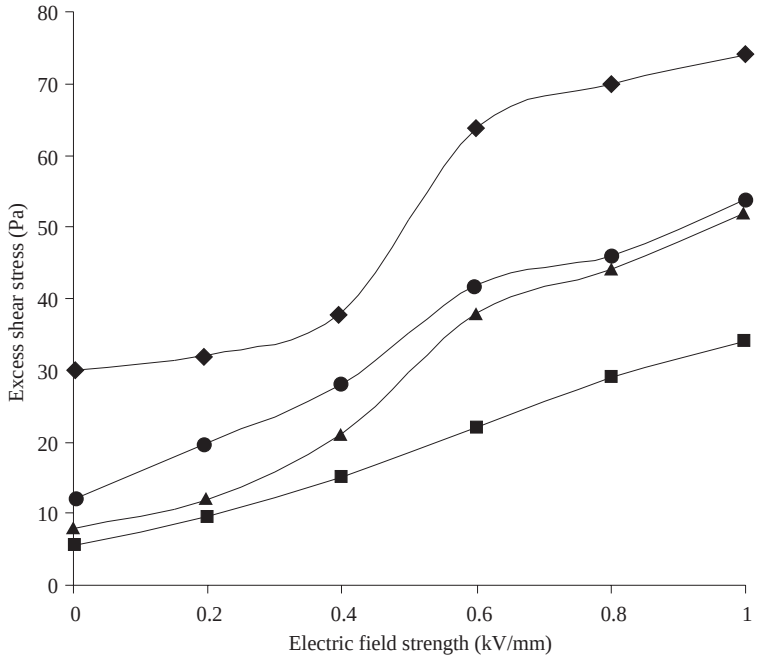

Figure 5. The changes in excess shear stress with electric field strength.
$\dot{\gamma} = 20\ s^{-1}$, T = 20 °C, c = 20%, dispersion medium: (♦) SO, (●) DOP, (▲) TOTM, (■) MO.

Effects of shear rate and temperature on viscosity

The changes in logη with $\dot{\gamma}$ at 2 different temperatures (T = 20 and 80 °C) and electric field strengths (E = 0.0 and 1.0 kV/mm) are shown in Figure 6. As is evident, with and without applied electric field, that the viscosity of suspensions decreases sharply with increasing shear rate, giving a typical curve of shear thinning non-Newtonian[44] visco-elastic behaviour for both temperatures studied. These characteristic behaviours of the ER suspension are related to the internal particle structure induced by an applied electric field. Before shearing the ER fluid, the dispersed particles are aligned through the electric field direction making columnar structures, and these structures get stronger at higher electric fields, giving rise to increased viscosity of the ER fluids, as reflected in Figure 6. With increasing shear rate, the electric field induced fibrillar structure formed is destroyed, and resulting in decreased viscosity. Similar results were reported in studies of poly(naphthalene quinone radical)[43], polyaniline[45], magnesium hydroxide[46] and mesoporous molecular sieve[47], all of which were prepared in silicone oil.

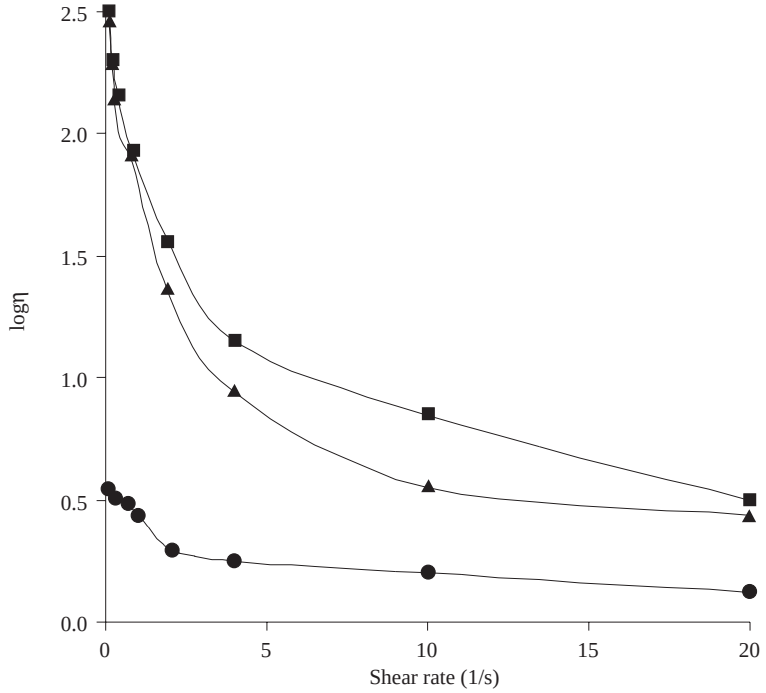

Figure 6. The changes in log(viscosity) with shear rate.
(■) 20 °C, E = 1.0 kV/mm; (▲) 80 °C, E = 1.0 kV/mm; (●) 20 °C, E = 0.0 kV/mm, c = 20 (m/m, %), dispersion medium: SO.

As reflected in Figure 6, high temperature caused a small decrease in the $\eta_{(E\neq 0)}$ of ionomer suspensions as the shear rate exceeds $\dot{\gamma}$ = 5 s^{-1}, whereas for the PI-co-PTBMA-Li/SO micellar system, no effect of temperature was observed on the $\eta^{29}_{(E\neq 0)}$. There may be 3 causes that change the ER effect substantially. The first is the viscosity loss of the dispersion medium at high temperature (η = 0.08 Pas at 20 °C and 0.06 Pas at 80 °C). The second is that temperature can definitely change the polarisability of the ER suspension. The third is that temperature would directly impact particle's thermal motion. If the Brownian motion were intensified at high temperatures and could become strong enough to compete with the electric field

induced fibrillar structure formed by the particles, the ER effect would become weaker. Whether temperature increases would intensify or weaken the ER effect is actually dependent on the factor that is dominant at that temperature[6].

On the other hand, an improved ER response was reported at higher temperatures in several ER suspensions, including both inorganic and polymeric systems[48−50]. The readily facilitated polarisation of the electric double layer in a hydrous (promoter activated) ER system was thought to contribute to the ER effect improvement at high temperatures, while the change in the particle's intrinsic property was thought to be responsible for the ER effect enhancement in an anhydrous (promoter free or dry-base) ER system[6].

Effect of moisture on ER activity

The influence of moisture on ER activity was also investigated by adding polar promoters (i.e. water, ethanol, ethanolamine, glycerol) at 100-1000 ppm (with 100 ppm increments) concentrations into PTBMA-Li suspensions at optimum concentration (c = 20 m/m, %). It was observed that the polymeric system studied in the present work was insensitive to the amount of moisture present over the range studied, the same as with the PI-co-PTBMA-Li/silicone oil system[28]. According to these results we may call the PTBMA-Li/silicone oil system a dry-base ER fluid. The variability of ER activity with temperature and moisture content is known to be a major problem with most conventional ER fluids and can limit their high temperature use[51]. It is generally thought that dry-base ER systems are superior to wet-base systems in their applications, due to their thermal and colloidal stabilities. The observation that the ionomer system investigated in the present work is not affected by the addition of polar promoter and high temperature could prove particularly important from an industrial and application point of view.

Conclusions

We have shown that poly(tert-butylmethacrylate) can be partially hydrolysed and converted to the Li salt. The colloidal stability of the ionomer in silicone oil was 32 days (c = 5%). Flow times of suspensions were observed to increase with increasing electric field strength and suspension concentration. The highest flow time was obtained as 32 s in silicone oil (c = 33%, E = 1.2 kV/mm). The electric field viscosity was found to increase up to 20% suspension concentration and then decrease. The ER activity of suspensions was observed to increase with increasing electric field strength, and ionomer concentration and with decreasing shear rate. Excess shear stress was found to increase sharply with increasing electric field strength and suspension concentration. The viscosity of suspensions decreased sharply with increasing shear rate, giving a typical shear-thinning non-Newtonian visco-elastic behaviour. It was found that the ionomer system studied in the present work was insensitive to high temperature and moisture within the limits studied. The performance of the insulating oils studied was in the order of SO > MO > TOTM > DOP.

Acknowledgement

We are grateful to the Scientific and Technical Research Council of Turkey (TUBITAK) (TBAG-1485) and Gazi University Research Fund (FEF-05/2003-21) for their financial support of this work.

References

1. T.C. Hasley, **Science, 25 (8)**, 761 (1992).
2. H. Block and J.P. Kelly, **J. Phys. D: Appl. Phys**., **21**, 1661 (1988).
3. C.J. Gow and C.P. Zukoski, **Adv. Colloid Interface Sci.**, **136**, 105 (1989).
4. H.Q. Xie, **J. Appl. Polym. Sci., 158**, 951 (1995).
5. Z.P. Shulman, R.G. Gorodkin, E.V. Korobko and V.K. Gleb, **J. Non-Newtonian Fluids Mechanics, 8**, 29 (1981).
6. T. Hao, **Adv. Colloid and Interface Sci.**, **97**, 1 (2002).
7. R. Tao and G.D. Roy, **Electrorheological Fluids: Mechanisms, Properties, Technology and Applications**, Eds. R. Tao and G.D. Roy, World Scientific London, 1994, chapter 4.
8. W.M. Winslow, **J. Appl. Phys., 20**, 1137 (1949).
9. A.P. Gast and C.F. Zukoski, **Adv. Colloid Int. Sci., 30**,153 (1989).
10. Y. Otsubo, M. Sekine and S. Katayama, **J. Rheol., 36**, 479 (1992).
11. G.B. Thurston and E.B. Gaertner, **J. Rheol., 35**, 1327 (1991).
12. S.G. Kim, J.W. Kim, W.H. Jang, H.J. Choi and M.S. Jhon, **Polymer, 42**, 5005 (2001).
13. H. Block, J.P. Kelly, A. Qin and T. Watson, **Langmiur, 35**, 687 (1990).
14. H.J. Choi, M.S. Cho, M.S. Jhon, **Int. J. Mod. Phys. B**, **13**, 1901 (1999).
15. J.H. Lee, M.S. Cho, H.J. Choi and M.S. Jhon, **Colloid Polym. Sci**., **73**, 277 (1999).
16. D. Quadrat, J. Stejskal, P. Kratochvil, C. Klason, D. McQueen, J. Kubat and P. Saha, **Synth. Met**., **37**, 97 (1998).
17. M.S. Cho, H.J. Choi and K. To, **Macromol. Rapid Commun**., **19**, 271 (1998).
18. H.J. Choi, J.W. Kim and K. To, **Synth Met**., **101**, 697 (1999).
19. J. Trlica, P. Saha, O. Quadrat and J. Stejskal, **Eur. Poly. J., 36**, 2313 (2000).
20. R. Bloodworth and E. Wendt, **Int. J. Mod. Phys B**., **10**, 2951 (1996).
21. H.J. Choi, J.W. Kim, M.H. Noh, D.C. Lee and M.S. Jhon, **J. Mater. Sci. Lett**., **18**, 1505, (1999).
22. J.W. Kim, H.J. Choi and M.S. Jhon, **Macromol. Symp**., **155**, 229, (2000).
23. J.W. Kim, S.G. Kim, H.J. Choi and M.S. Jhon, **Macromol. Rapid Commun**. **20**, 450 (1999).
24. B.H. Kim, J.H. Jung, J. Joo, J.W. Kim and H.J. Choi, **J. Korean Phys. Soc**. **36**, 366 (2000).
25. H.Q. Xie, D. Tian, P. He and J. Guo, **J. Appl. Polm. Sci., 68**, 2169 (1998).
26. H.I. Unal and H. Yilmaz, **J. Appl. Polym. Sci**., **86**, 1106 (2002).
27. M. Yavuz, H.I. Unal and Y. Yildirir; **Turk. J. Chem., 25**, 19 (2001).
28. M. Yavuz and H.I. Unal **J. Appl. Polym. Sci., 91,** 1822 (2004).
29. J.F. Watts and T.J.Carney, **Powder Metallurgy-An Overview, The Institute of Materials,** London UK, 28-81, (1991).
30. D. Sahin, B. Sari and H.I. Unal, Turk. J. Chem., **26**, 113 (2002).

31. V.I. Bezruk, A.N. Lazarev, V.A. Malov and O.G. Usyarov, **Coll. J., 34**, 142 (1972).

32. S. Wu and J. Shen, **J. Appl. Polym. Sci., 60**, 2159 (1996).

33. V.I. Kordonsky, E.V. Korobko and T.G. Lazareva, **J. Rheol., 35**, 1427 (1991).

34. C. Gow and C.F. Zukoski, **J. Colloid Interface Sci., 136**, 175 (1990).

35. T. Dürrschmidt and H. Hoffmann, **Colloids and Surfaces, A: Physicochemical and Enginering Aspects, 156,** 257 (1999).

36. I.K. Yang and I.T. Huang, **J. Polym Sci. Part B Polym. Phys., 35 (8)**, 1217 (1997).

37. A. Lengalova, V. Pavlinek, P. Saha, J. Stejskal and O. Quadrat, **J. Colloid Interface Sci., 258**, 174 (2003).

38. J.B. Yin and X.P. Zhao, **J. Colloid Interface Sci.** 257, 228 (2003).

39. D.J. Klingenberg and C.F. Zukoski, **Langmiur, 6**, 15 (1990).

40. Y. Xu and R. Liang, **J. Rheol., 35,** 1355 (1991).

41. G. Bossis, E. Lemaire, O. Volkova and H. Clercx, **J. Rheol**., 35, 687 (1997).

42. J.N. Foulc and D. Atten, **Electrorheological Fluids: Mechanism, properties, technology and applications,** Eds. R. Tao and G.R. Roy, World Scientific, London, (1994) p. 358-371.

43. M.S. Cho and H.J Choi, **Korea-Australia Rheol. J., 12 (3,4)** 151 (2000).

44. K.D. Weiss and T.G. Duclos, "**Controllable Fluids: The temperature dependence of post-yield properties**" in **Electrorheological Fluids: Mechanisms, Properties, Technology and Applications**, Eds. R. Tao and G.D. Roy, World Scientific, London, 1994, pp. 43-59.

45. K. Tanaka and Y. Orwa, **Polymer, 30**, 171 (1998).

46. H.P. Gavin, **J. Non-Newtonian Fluid Mechanics, 71**, 165 (1997).

47. H.J Choi, M.S. Cho, K.K. Kang and W.S. Ahn, **Microporous and Mesoporous Materials, 39**, 19 (2000).

48. D.L. Klass and T.W. Martinek, **J. Apll. Phys., 38**, 67 (1967).

49. D.L Klass and T.W. Martinek, **J. Apll. Phys., 38**, 75 (1967).

50. U.Y. Treasurer, F.E. Filisko and L.H. Radzilowski, **J. Rheol**., **35**, 1051 (1991).

51. P.J. Rankin and D.J. Klingenberg, **J. Rheol.**, **42**, 639 (1998).